

Upper-twin-peak quasiperiodic oscillation in x-ray binaries and the energy from tidal circularization of relativistic orbits

C. Germanà*

Departamento de Física, Universidade Federal do Maranhão, São Luís, MA, Brazil

(Dated: October 28, 2018)

High frequency quasiperiodic oscillations (HF QPOs) detected in the power spectra of low mass x-ray binaries (LMXBs) could unveil the fingerprints of gravitation in strong field regime. Using the energy-momentum relation we calculate the energy a clump of plasma orbiting in the accretion disk releases during circularization of its slightly eccentric relativistic orbit. Following previous works, we highlight the strong tidal force as mechanism to dissipate such energy. We show that tides acting on the clump are able to reproduce the observed coherence of the upper HF QPO seen in LMXBs with a neutron star (NS). The quantity of energy released by the clump and relativistic boosting might give a modulation amplitude in agreement with that observed in the upper HF QPO. Both the amplitude and coherence of the upper HF QPO in NS LMXBs could allow us to disclose, for the first time, the tidal circularization of relativistic orbits occurring around a neutron star.

PACS numbers: 95.30.Sf, 97.80.Jp, 97.10.Gz

I. INTRODUCTION

The twin-peak high frequency quasiperiodic oscillations (HF QPOs), observed in the power spectra of low mass x-ray binaries (LMXBs) with either a neutron star (NS) or a black hole (BH), could carry information on the matter orbiting in the accretion disk around the compact object. Their central frequencies are typical of the orbital motion close to the compact object. HF QPOs are potential probes to prove the laws of gravitation close to a NS or a BH [1]. The first-discovered twin-peak HF QPOs were observed with central frequency up to ~ 1130 Hz in a NS LMXB [2]. They were named twin-peak kilohertz QPOs because they often show up in pairs. The HF QPOs observed in BH LMXBs have frequencies of hundreds of hertz [3, 4] and show different features than HF QPOs seen in NS LMXBs. While in NS LMXBs the central frequency of the peaks is seen to vary, in BH LMXBs the twin-peak HF QPOs are observed at fixed frequencies, showing a cluster at the 3:2 frequency ratio. The clustering has motivated models proposing that HF QPOs might be related to resonance mechanisms of the matter orbiting in the curved space-time [5–9]. The HF QPOs in BH LMXBs have a coherence lower than in NS LMXBs and an amplitude not displaying the characteristic patterns seen in NS LMXBs (e.g. Refs. [10, 11]). Low frequency QPOs (< 100 Hz) seen in both NS and BH LMXBs may be related to relativistic frame dragging around the spinning compact object [12], a prediction of general relativity (GR) in strong field. The effect on the orbiting matter is known as Lense-Thirring precession [13]. Recent works have put forward strong evidence that the low frequency QPO seen in the BH LMXB H1743-322 is produced by frame dragging [14, 15]. In the case of NS LMXBs, recent data analysis shows that the predic-

tions of the modeling differ from the data because other factors may affect the modulation mechanism [16].

Other GR effects potentially detectable around the compact object in LMXBs are, e.g., the periastron precession of the orbits [17] occurring on milliseconds time-scale as well as the existence of an innermost stable bound orbit (ISBO) [18, 19]. The unprecedented opportunity to disclose such phenomena in the imprints left by the HF QPOs has stimulated several works on the modulations that would be produced by matter orbiting around a compact object [20–23]. Ray-tracing of the photons emitted by an overbright hot-spot orbiting a Kerr black hole shows the signal that a distant observer would see [22]. The light curve produced by the hot-spot is modulated at its orbital period because of relativistic effects. Increasing the inclination towards an edge-on view, the light curve becomes sharper because of increasing Doppler boosting and gravitational lensing. The power spectrum of the signal from a slightly eccentric orbit ($e \sim 0.1$) shows several peaks: the keplerian frequency ν_k , the radial frequency¹ ν_r , the beats $\nu_k \pm \nu_r$ and their harmonics. Also, the authors have simulated the signal emitted by an arc sheared along the orbit. The power spectrum shows pronounced peaks at ν_k and $\nu_k \pm \nu_r$ and much less power at the harmonics.

Ray-tracing presented in Ref. [23] shows the different detectability that HF QPOs would have between current and future x-ray satellites, taking into account also the radial drift of the accreting hot-spot. In the power spectra the peaks and harmonics at ν_r , ν_k and $\nu_k + \nu_r$ (or $2(\nu_k - \nu_r)$) are detected. Differences between the signal from the orbiting hot-spot and the one from axisymmetric disk oscillations are investigated as well.

In a more dynamical framework, in Refs. [24, 25] were

¹ The radial frequency ν_r is the frequency of the cycle from periastron of the orbit to apastron and back to periastron. In a curved space-time $\nu_r \neq \nu_k$.

* claudio.germana@gmail.com; claudio.germana@ufma.br

introduced ray-tracing techniques in the case of clumps of matter stretched by the strong tidal force around a Schwarzschild black hole. Differently than the rigid hot-spot case, the stretching of the clump, as long as it orbits, leads to a sudden increase of its luminosity producing a power law in the power spectrum [25, 26]. Moreover, the stretching blurs the signal emitted in the case of a rigid sphere or a circular hot-spot. This implies some peaks and harmonics not be detected in the power spectrum. In other works the stretching of the clump is simulated as an arc along the orbit, in order to get power spectra with few peaks as in the observations. In the tidal model the stretching is a natural consequence of tidal deformation of the clump. The simulation using a slightly eccentric orbit ($e = 0.1$) gives a power spectrum with a power law and two peaks, as in the observations [3]. The lower peak in frequency corresponds to ν_k , the upper one to the beat $\nu_k + \nu_r$ [26]. Tidal disruption events have already been recognized in the case of stars disrupted by supermassive black holes (e.g. Refs. [27–30]). Efforts to model such events are going forward in the details (e.g. Refs. [31–34]). QPOs have been detected in the energy flux of some tidal disruption events [35, 36]. Tidal interaction is a mechanism that can provide significant amounts of energy. In our neighborhood, some moons display geological activities whose energy is pumped by the tidal force of the parent planet: the strongest volcanism in Jupiter’s moon Io [37] and possibly the discovered ocean [38, 39] and geothermal activity in Saturn’s moon Enceladus [40, 41]. Thus, the strong tidal force by the compact object in LMXBs, acting on clumps of plasma orbiting in the accretion disk, may be a valid ingredient to model the main features observed in twin-peak HF QPOs.

A planet/moon orbiting the central object on an eccentric orbit dissipates its orbital energy because of tides and its orbit gets circular [42]. In Ref. [43] has been shown that the orbit of a low-mass satellite around a Schwarzschild black hole circularizes and shrinks because of tides. Energy is transferred from orbit to internal energy of the satellite. The energy emission mechanism that would turn the released orbital energy into electromagnetic radiation has been investigated in Refs. [25, 44]. The authors show that it may be x-ray radiation from synchrotron mechanisms if the clump of plasma is permeated by a magnetic field. In Ref. [45] the authors conclude that magnetically confined massive clumps of plasma might form in the inner part of the accretion disk. In Ref. [46] it is shown that the hard x-ray radiation, over 10-100 milliseconds time intervals, observed in two x-ray binaries is better interpreted through cyclo-synchrotron self-Compton mechanisms. The calculations in Refs. [25, 44] show that during tidal stretching the magnetic field could largely increase. Moreover, gravitational energy extracted through tides might go into kinetic energy of the electrons in the plasma, since the clump is rapidly expanding into a pole. This mechanism could provide relativistic electrons emitting syn-

chrotron radiation. Magnetohydrodynamics simulations are required to know how this mechanism actually works. Recent numerical simulations of the magnetic field in a star disrupted by tides [34] show a magnetic field largely increasing, as from the calculations in Refs. [25, 44].

The emission of radiation because of the orbital energy released during tidal circularization of the orbit thus would cause an overbrightness of the clump with respect to the background radiation from the disk. In Ref. [47] has been shown that the timing law of the azimuth phase $\phi(t)$ on a slightly eccentric relativistic orbit produces multiple peaks in the power spectrum: the keplerian frequency ν_k and the beats $\nu_k \pm \nu_r$. The beats $\nu_k \pm \nu_r$ are produced because of the eccentricity of the orbit. The orbiting body has a different orbital speed at periastron and apastron passage, happening at the frequency $\nu_r \neq \nu_k$ in the curved space-time. This introduces a modulation in the phase $\phi(t)$ at the relativistic radial frequency ν_r . In the case of a circular orbit (in every case in a flat space-time) only the peak at ν_k is produced. As already mentioned above, the timing law $\phi(t)$ turns into a modulated observable light curve because of relativistic effects on the emitted photons [22, 23, 25]. The amplitude of the beats $\nu_k \pm \nu_r$ thus originates because of the orbital energy released during tidal circularization of the orbit. Moreover, the coherence of the beats is related to the time-scale the circularization takes place, since once the orbit is circular or quasi-circular the beats $\nu_k \pm \nu_r$ fade and the emitted energy is modulated only at the keplerian frequency ν_k .

Most efforts to interpret the twin-peak HF QPOs have focused on the identification of their central frequencies with those of the orbital modes in the curved space-time. The proposed models link the upper HF QPO of the twin-peaks to the keplerian modulation ν_k produced by a clump of plasma orbiting in the accretion disk, other models link the lower HF QPO to ν_k [20–22, 48–50]. On the other hand, attempting to interpret the amplitude and coherence of HF QPOs might disclose useful information on their nature as well. In Refs. [51–54] are reported both the amplitude and coherence of the twin-peak HF QPOs observed in NS LMXBs. The behavior of the amplitude as a function of the central frequency of the peaks shows characteristic patterns in atoll NS LMXBs [55]. The amplitude of the upper HF QPO displays a decrease with increasing central frequency of the peak, instead the amplitude of the lower HF QPO shows an increase and then a decrease. The coherence Q of the lower HF QPO ($Q = \nu/\Delta\nu$ with ν central frequency and $\Delta\nu$ full width at half maximum of the peak) shows a characteristic pattern too: Q as a function of ν increases and then drops abruptly [52–54]. In Ref. [52] has been underlined that the abrupt drop of Q , seen in several atoll NS LMXBs, could be a signature of the oscillation approaching the ISBO predicted by GR. This relevant issue was subsequently discussed with extensively data analysis in Refs. [53, 54]. Although the excursion of Q of the lower HF QPO is more than an order of magnitude, the Q of the upper HF QPO shows an almost flat trend

over a large range of frequencies, mostly remaining of the order of $Q \sim 10$.

In a previous work (Ref. [56], hereafter GC15) we have proposed that the amplitude and coherence of the lower HF QPO might originate from the energy released by a clump of plasma spiraling to inner orbits because of the work done by the tidal force, dissipating the orbital energy. In this paper we aim to investigate on the amplitude and coherence of the upper HF QPO [52]. Here is proposed that the upper HF QPO might originate from the energy released during tidal circularization of the clump's orbit. In Ref. [43] has been shown that the orbit of a clump of matter orbiting a Schwarzschild black hole circularizes and shrinks because of tides. The release of orbital energy during circularization of the orbit might provide the overbrightness of the clump required in order to produce detectable modulations [22, 25]. The emitted photons are modulated at ν_k and $\nu_k \pm \nu_r$ in the power spectrum [22, 47]. The beats $\nu_k \pm \nu_r$ should show up only in the phase of tidal circularization of the orbit, since once the orbit gets circular $\nu_k \pm \nu_r$ fade and the emitted radiation is modulated only at ν_k . Tidal disruption simulations show an upper HF QPO corresponding to the beat $\nu_k + \nu_r$ [26]. Therefore, we believe and inspect that both the amplitude and coherence of the upper HF QPO in the observations [52] should be reproduced by the energy released during tidal circularization of relativistic orbits.

The paper is organized as follows. In Section II we recall the main arguments described in GC15 about the tidal load on clumps of plasma orbiting in the accretion disk. In Section III we explore the idea presented in this manuscript, i.e. the amplitude and coherence of the upper HF QPO seen in NS LMXBs could be related to the energy released during tidal circularization of relativistic orbits. We estimate the energy released by an orbiting clump of plasma when its slightly eccentric orbit gets circular. We use the energy-momentum relation in the Schwarzschild metric² since it is the relativistic equation that embeds all the contributions to the total energy of an orbiting clump of matter. The time-scale of tidal circularization of the orbit is calculated. Afterwards, we calculate the coherence Q the produced beat $\nu_k + \nu_r$ would have. We compare it to the upper HF QPO coherence pattern seen in the observations (e.g. Fig. 2 in Ref. [52]). In Section IV we attempt to tie the orbital energy released³ during circularization of the orbit to the observable fraction of energy modulated by Doppler boosting.

We follow the detailed results in Ref. [22] to get the observable amplitude of the beat $\nu_k + \nu_r$. In Section V we discuss the results in this paper in light of other theoretical and observational results. Section VI summarizes the conclusions.

II. ORBITING CLUMPS OF PLASMA AND TIDAL LOAD

Motivated by the results from tidal disruption of clumps orbiting a Schwarzschild black hole [24, 25], reproducing power spectra much alike to the observed ones [26], in GC15 we have estimated the energy coming from the tidal disruption of a clump of plasma in the accretion disk around LMXBs. Magnetohydrodynamics simulations show that the inner part of the accretion disk is highly turbulent [58]. In Ref. [59] the authors reported the discover of large structures in the accretion disk of a x-ray binary. Propagating accretion rate fluctuations in the disk are modeled [60, 61] to reproduce the aperiodic variability observed in BH LMXBs. Thus, it is hard thinking to a smooth accretion disk, but rather it may be characterized by inhomogeneities propagating throughout it. Note that in Ref. [45] is shown that magnetically confined massive clumps of plasma might form in the inner part of the accretion disk. In light of this, in GC15 we explored the idea of treating a clump of plasma as characterized by some internal force keeping the clump together (e.g. electrochemical bounds and/or magnetic forces). In this section we recall the main arguments in GC15.

A spherical clump of radius R , mass μ and density ρ undergoes a tidal force (between two opposite spherical caps of the clump, at $r - R$ and $r + R$; see also GC15)

$$F_T = \mu' c^2 \left[\left(\frac{dV_{eff}}{dr} \right)_{(r-R)} - \left(\frac{dV_{eff}}{dr} \right)_{(r+R)} \right] \quad (1)$$

$$\approx \mu' c^2 2R \left(\frac{d^2 V_{eff}}{dr^2} \right)_r$$

where $\mu' = \rho V'$ is the mass of the spherical cap, of height, say, one tenth of the radius, $h = R/10$. The volume of the cap is $V' = \pi h^2 (R - h/3)$. V_{eff} in (1) is the gravitational effective potential in the Schwarzschild metric (7). In the case of a solid-state clump of matter, the clump is kept together by an internal force (electrochemical bounds) characterized by the ultimate tensile strength σ , i.e. the internal force per unit area. The tidal force has to be weaker than internal forces, $F_T \leq 2\pi R h \sigma$. From this inequality we can get some order of magnitude on the

² We use the Schwarzschild metric because there are in the literature exact parametrization of both the orbital energy E and angular momentum L per unit mass, for a test-particle on an orbit with generic eccentricity e [57].

³ We emphasize that the main goal of the manuscript is to justify how (from where) the amount of energy carried by the detected upper HF QPO would originate. We estimate the amount of the bolometric energy that would be released by this mechanism, to compare it to the bolometric energy observed in the upper

HF QPO. Here our main purpose is not the spectral energy distribution (i.e. how the orbital energy then is emitted), which depends on the exact energy emission mechanism (see Sec. IV for a discussion on this point).

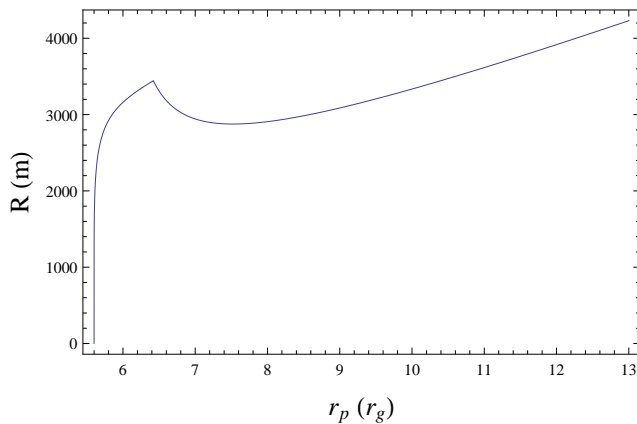


FIG. 1. Radius R set by tides of a clump of plasma as a function of the periastron of the orbit r_p , around a $2 M_\odot$ neutron star.

maximum radius R_{max} set by tides ⁴

$$R_{max} = \left(10 \left(1 - \frac{1}{30} \right)^{-1} \frac{c_s^2 \sigma}{c^2 Y} \times \left(-\frac{2m}{r^3} + \frac{3\tilde{L}^2}{r^4} - \frac{12m\tilde{L}^2}{r^5} \right)^{-1} \right)^{1/2} \quad (2)$$

where we wrote the density $\rho = c_s^2/Y$, Y is the Young's modulus of the material, c_s the speed of sound in it. As mentioned above, in Section IV of GC15 we explored the idea of treating clumps of plasma in the accretion disk as characterized by some internal force per unit area σ (electrochemical bounds and/or magnetic forces). The speed of sound in the plasma is [63]

$$c_s = \left(\frac{\gamma Z k T}{m_i} \right)^{1/2} \quad (3)$$

where $\gamma \sim 5/3$ is the adiabatic index, Z the charge state ($Z = 1$ for a hot plasma), m_i the ion hydrogen mass, k the Boltzmann's constant [63].

In GC15 we pointed out that clumps with $R = R_{max}$ would not probably form at all because of tides. The tidal load (the tidal force (1) per unit area) has to be n times smaller than σ , i.e. $F_T/2\pi R h = \sigma_T = \sigma/n$, where

$$\sigma_T = \frac{\mu' c^2}{2\pi R h} \left[\left(\frac{dV_{eff}}{dr} \right)_{(r-R)} - \left(\frac{dV_{eff}}{dr} \right)_{(r+R)} \right] \quad (4)$$

$$\approx \frac{10\mu' c^2}{\pi R} \left(\frac{d^2 V_{eff}}{dr^2} \right)_r$$

⁴ Note that the R_{max} calculated in GC15 in the case of a solid-state clump agrees to the dimensions derived in Ref. [62] of a bar falling into a gravitational field.

In GC15 we constrained $n = 5$ as upper limit, giving $R \sim 3000$ m. A larger n implies a clump with radius R emitting gravitational energy lower than that observed in HF QPOs ($\approx 10^{35} - 10^{36}$ erg/s). On the other hand, a smaller n gives larger radii R , close to R_{max} . As mentioned above, such clumps would not probably form/survive at all because of tides. Fig. 1 shows the radius $R = R_{max}/\sqrt{5}$ set by tides (from equation (2)) as a function of the periastron r_p of the orbit, in the case $\sigma_T = \sigma/5$. In (2) the ratio σ/Y was constrained in GC15 (equation (9)) and is $\sigma/Y = 300$ in atoll sources ($\sigma/Y = 70$ in Z-sources; see Section VII B in GC15). The speed of sound c_s is from (3). In Fig. 1 we see that, as long as the tidal force strengthen towards the inner regions, R decreases as expected. However, getting closer to ISBO ($r \sim 5.6 r_g$) R increases and then drops. The slightly increase is caused by the weakening of the tidal force close to ISBO. Close to ISBO the gravitational potential (7) flattens and, therefore, the tidal force weaken. This can be seen in Fig. 2. It shows the tidal load σ_T (4) in Pascal on a clump of plasma $R = 3000$ m big for several orbits of different periastron. Over each orbit (each segment in the figure) σ_T changes from the periastron to the apastron of the orbit. Its overall behavior increases and then drops close to ISBO because of the flattening of the potential. The flattening of the minimum of the potential V_{eff} is a features of GR [18] and causes the decrease of the difference of potential energy between close orbits reported in GC15.

The drop of R in Fig. 1 close to ISBO is caused by the drop at ISBO (inner edge of the accretion disk) of the speed of sound in the plasma (see equation (2)). The cusp seen at $r_p \sim 6.4 r_g$ is because of the orbit at which the tidal force is almost equal at periastron and apastron. Orbits with bigger radii have the tidal force stronger at periastron, as expected, therefore we calculate the radius R of the clump set by tides at periastron. However, orbits with r smaller than $r \sim 6.4 r_g$ have a tidal force stronger at apastron, because of the flattening of the potential. This can be seen in Fig. 2. Thus, we calculate the radius R set by tides at the apastron of the orbit.

The patterns in both figures are for orbits of eccentricity⁵ $e = 0.1$, for a neutron star of $2 M_\odot$ and an accretion rate of $\dot{M} \sim 7 \times 10^{16}$ g/s, giving the luminosity observed in atoll sources, i.e. $L \sim 0.07 L_{Edd} \sim 10^{37}$ erg/s ([64], where $L_{Edd} \sim 2.5 \times 10^{38}$ erg/s is the Eddington lumi-

⁵ It might be reasonable thinking that during accretion a clump of plasma may have a trajectory on a not perfect circular orbit, because of the turbulent environment [58]. Numerical simulations in Ref. [22] reproduce multiple peaks in the power spectrum, at ν_k and the beats $\nu_k \pm \nu_r$, for orbits with small eccentricity ($e \sim 0.1$). In Ref. [26] the upper HF QPO at $\nu_k + \nu_r$ in the power spectrum from numerical simulations is reproduced for an orbit with eccentricity $e = 0.1$. Such results [22, 26], much alike to observations, suggest that clumps on orbit with low e may exist in the disk. So here we chose $e = 0.1$, also to pursue the results reported in GC15 and Ref. [47].

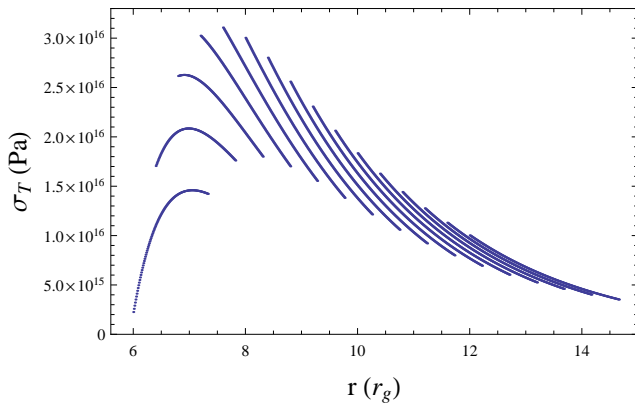


FIG. 2. Tidal load σ_T (4) over a clump of plasma $R = 3000$ m big as a function of the orbital radius. Each segment draws the variation of the load from periastron to apastron of the orbit.

nosity for a $\sim 2 M_\odot$ neutron star [63]). This accretion rate gives a density of the clump of plasma in the accretion disk of $\rho \sim 1$ g/cm³ and the speed of sound in it $c_s \sim 4 \times 10^7$ cm/s [63].

III. THE ENERGY AND TIME-SCALE FROM TIDAL CIRCULARIZATION OF RELATIVISTIC ORBITS

The total energy of an orbiting test-particle of mass μ is enclosed in the energy-momentum relation⁶

$$g_{\alpha\beta} p^\alpha p^\beta = -\mu^2 \quad (5)$$

with $g_{\alpha\beta}$ metric tensor and $p^{\alpha(\beta)}$ contravariant four-momentum of the test particle [18]. In the Schwarzschild metric substituting the $p^\alpha = dx^\alpha/d\tau$ (τ proper time; see e.g. [57]) and extending (5) we get

$$\tilde{E}^2 = \left(\frac{dr}{d\tau}\right)^2 + \left(1 - \frac{2m}{r}\right) \left(1 + \frac{\tilde{L}^2}{r^2}\right) \quad (6)$$

m is the mass of the compact object⁷, \tilde{E} and \tilde{L} total energy and angular momentum per unit mass μ of the test-particle, r is the radial coordinate. Equation (6) (whose square root, multiplied by μc^2 , we can write as $E = \mu_{rel} c^2$, with μ_{rel} relativistic mass) tells us the energy contributions to the total energy \tilde{E} . The first term is the energy coming from the radial motion, i.e. the motion

from periastron to apastron and back to periastron. The second term is the effective gravitational potential [57]

$$V_{eff} = 1 - \frac{2m}{r} - \frac{2m\tilde{L}^2}{r^3} + \frac{\tilde{L}^2}{r^2} \quad (7)$$

with contribution from the rest-mass energy (per unit mass μ), the gravitational and centrifugal potential.

In Ref. [57] are reported exact parametrization for the total (or orbital) specific energy \tilde{E} and specific angular momentum \tilde{L} , for a generic orbit of semi-latus rectum p and eccentricity e

$$\tilde{E}(p, e) = \left(\frac{(p-2-2e)(p-2+2e)}{p(p-3-e^2)}\right)^{1/2} \quad (8)$$

$$\tilde{L}(m, p, e) = \left(\frac{p^2 m^2}{p-3-e^2}\right)^{1/2} \quad (9)$$

p is linked to the periastron r_p of the orbit through $r_p = pm/(1+e)$.

The energy (in international system units) that a clump of matter of mass μ would release, if its orbit of eccentricity e is circularized, is from (8)

$$\epsilon = \mu c^2 \left(\tilde{E}(p, e) - \tilde{E}(p, 0)\right) \quad (10)$$

We aim to compare the released energy ϵ to the energy (amplitude) carried by the upper HF QPO observed in NS LMXBs (Fig. 3 in Ref. [52]). The upper HF QPO of the twin-peaks corresponds to the beat $\nu_k + \nu_r$ in the power spectrum from numerical simulations [26, 47]. This beat is caused by the eccentricity of the orbit and originates only in the phase of tidal circularization of the orbit, when energy is released and it is modulated at $\nu_k + \nu_r$, till the orbit gets circular, then $\nu_k + \nu_r$ fades.

We calculate the relativistic keplerian⁸ ν_k and radial ν_r frequency as in Ref. [47], for an orbit with eccentricity $e = 0.1$. Fig. 3 shows the orbital energy released ϵ (10) to circularize the orbit of initial $e = 0.1$ as a function of the frequency of the beat $\nu_k + \nu_r$, i.e. for clumps orbiting at different orbital radii. The range of orbital radii is $\sim 6 r_g$ to $13 r_g$. At each orbital radius the clumps have R as in Fig. 1. The energy released corresponds to $\sim 0.3\%$ μc^2 . We see that the energy released when, e.g., $\nu_k + \nu_r \sim 520$ Hz ($r_p \sim 13 r_g$) is higher than that released by a clump orbiting at $r_p \sim 7 r_g$ ($\nu_k + \nu_r \sim 1100$ Hz). Close to ISBO it drops.

With the amount of orbital energy released by the clump to circularize its orbit we can investigate whether the upper HF QPO seen in the observations could actually

⁶ Hereafter we use geometric units ($G = c = 1$), unless differently specified.

⁷ The mass m in geometric units is equal to the gravitational radius of the compact object $r_g = GM/c^2$, where M is the mass of the compact object in international system units, G the gravitational constant and c the speed of light. For a $2 M_\odot$ neutron star $r_g \sim 3$ km.

⁸ We would warn that keplerian motion for matter orbiting close to a neutron star is an approximation, since the effects of a boundary layer might deviate the orbital motion from purely keplerian.

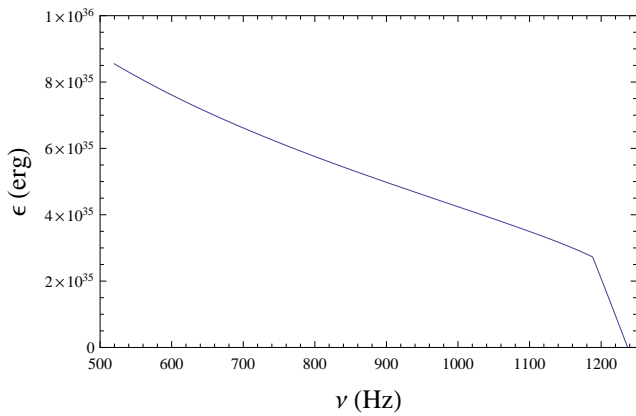


FIG. 3. Orbital energy released by a clump of plasma with R as in Fig. 1 in order to circularize its orbit with initial $e = 0.1$. The energy is plotted as a function of the frequency of the beat $\nu_k + \nu_r$ for a $2 M_\odot$ compact object.

originate from tidal circularization of relativistic orbits. We calculate the time-scale the circularization of the orbits by tides would take place. Then we compare the derived coherence of $\nu_k + \nu_r$ to the coherence behavior of the upper HF QPO observed in several atoll NS LMXBs (Fig. 2 in Ref. [52]).

The tidal force removes energy from orbit and loads it on the clump (e.g. Ref. [43, 65]). We aim to estimate the energy loaded by tides on the clump over one radial cycle, from periastron to apastron and back to periastron (see Fig. 2). To get order of magnitude, we substitute into (4) the parametrized radius $r(\chi) = pm/(1 + e \cos(\chi))$ as a function of the radial phase χ [57]. The tidal load (4) as a function of χ , which is an energy per unit volume, is integrated over one radial cycle χ , from periastron ($\chi = 0$) to apastron ($\chi = \pi$) and back to periastron ($\chi = 2\pi$). We multiply for the volume of the clump to get the energy loaded by tides per periastron passage. For a clump with R as in Fig. 1 and a density of the plasma typical for an atoll source ($\rho \sim 1 \text{ g/cm}^3$), the estimated amount of energy is of the order of ⁹ $E_{\text{tide}} \sim 10^{35}$ erg. We divide ϵ from (10) by E_{tide} (as a function of the orbital radius) to get the number of periastron passages N in order to circularize the orbit. The time it takes to circularize the orbit then is $t' = N/\nu_r$, equal to¹⁰ $t' \sim 0.01$ s at $r \sim 8 r_g$. The coherence of the beat $\nu_k + \nu_r$ is $Q = (\nu_k + \nu_r)/\Delta\nu = (\nu_k + \nu_r)t'$. Fig. 4 shows the coherence Q obtained from our calculations as a function of the frequency $\nu_k + \nu_r$. Like in Fig. 3, the range of frequency corresponds to a range of orbital radii of $\sim 13 - 5.6 r_g$. The radius R of the clump is shown in Fig. 1. The coherence Q is mostly constant and of the order of 10. Both

⁹ Note that the order of magnitude obtained $E_{\text{tide}} \sim 0.1\% \mu c^2$ agrees to that calculated with other formalisms in the case of a star disrupted by a supermassive black hole [31].

¹⁰ This time-scale is in agreement with that from the calculations in Ref. [43].

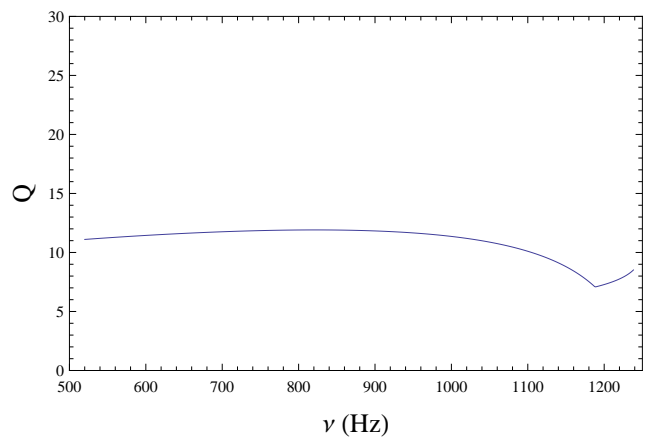


FIG. 4. Simulated coherence Q of the beat $\nu_k + \nu_r$ as a function of the frequency $\nu_k + \nu_r$ for a $2 M_\odot$ compact object. The value of Q is related to the time scale the tidal circularization of relativistic orbits takes place, for clumps of plasma of R as in Fig. 1. Such behavior is typical of the Q of the detected upper HF QPO. For a comparison with the data see Fig. 2 in Ref. [52]

its value and trend are much alike to the coherence of the upper HF QPO observed in NS LMXBs, Fig. 2 of Ref. [52] (filled star symbols). In Fig. 2 of Ref. [52] Q is of the order of $Q \sim 10$ for most of the sources.

We see that the Q calculated here strongly depends on the radius R of the clump, $Q \propto R^{-2}$. It may be worth emphasizing that the R in Fig 1 is derived from the calculations in Section II and the way to derive it was described in Sections III, IV in GC15. We are not assuming an R to match the Q from the observations, but its value is derived from calculations. This may be a significant result within this framework. Indeed, from the calculated R this approximated modeling is able to give for the first time both Q and the amplitude of the upper HF QPO (see Sec. IV) in agreement with those from observations [52].

IV. TYING THE RELEASED ORBITAL ENERGY TO THE OBSERVABLE AMPLITUDE OF THE MODULATION

The orbital energy released during tidal circularization of the orbit (eq. 10) gives time-scales of dissipation in agreement with the coherence Q of the upper HF QPO detected in atoll NS LMXBs [52]. However, this released orbital energy has to be converted somehow to electromagnetic radiation in order the upper HF QPO to be detected. Moreover, only a fraction of this radiation is modulated by Doppler boosting and detectable as HF QPOs [22]. In this section we discuss how the extracted orbital energy by tides would turn into radiation emitted by the clump (see footnote 3). We also estimate the amount of energy that would be modulated by Doppler

boosting and detected as a QPO, following the results in Ref. [22].

From the energy emission spectra of LMXBs we know that HF QPOs are observed in hard x-ray, their amplitude keep increasing towards hard x-ray (> 5 keV [66]). This means that the only thermal emission from the disk (soft x-ray, ~ 1 keV) can not justify their nature. A corona of hot electrons and/or a boundary layer contribute to the energy emission spectra observed in LMXBs (see e.g. Refs. [67, 68]). These components produce the hard x-ray spectrum seen in LMXBs. The soft x-ray photons from the disk are inverse-Compton scattered to higher energy by the corona and/or the boundary layer. There are evidences that the same mechanism could amplify the amplitude of the HF QPOs at hard x-ray [69, 70]. That is, the HF QPOs could be produced in the disk, but then they are amplified to hard x-ray by the corona and/or the boundary layer. It was recently suggested that the occurrence of the lower HF QPO could be because of some resonance between the comptonising medium and the accretion disk and/or the neutron star surface [71]. On the other hand, in Ref. [72] it is shown, by means of Monte Carlo ray-tracing, that multiple scattering of soft photons from the disk in a corona of hot electrons would smooth the oscillation that originates in the disk. In Ref. [72] it is suggested that it is unlikely that the same mechanism would produce HF QPOs at hard x-ray, since the emerging hard x-ray suffered more scattering than soft x-ray, thus the oscillation has a low amplitude at high energy bands (see Fig. 5 in Ref. [72]). It is also suggested that there may be in the disk a hot-spot already emitting hard x-ray photons, such that they are moderately scattered by the surrounding corona. In Ref. [46] the authors studied the energy spectra of two x-ray binaries over 10–100 ms time-scales. They concluded that the hard x-ray radiation is better explained through cyclo-synchrotron self-Compton mechanisms. Thus, if clumps of plasma in the accretion disk are permeated by some magnetic field, tidal stretching of the clump may provide a mechanism to produce non-thermal electromagnetic radiation. The orbital energy extracted through tides (e.g. Fig. 3) is transferred into internal energy of the clump (e.g. Refs. [43, 65]). In Refs. [25, 44] it is shown that during tidal stretching the magnetic field could largely increase. The extracted orbital energy could go into kinetic energy of the electrons in the plasma, since the clump is rapidly expanding into a pole. This mechanism could provide relativistic electrons winding around the magnetic field of the clump and producing synchrotron radiation [25, 44]. Synchrotron radiation by compact hot-spots has already been proposed as mechanism to produce the hard x-ray spectrum seen in HF QPOs [73]. It is clear that full magnetohydrodynamics simulations are required to see how the clump disrupted by tides would emit its energy. On the other hand, we have some clues which could be used to estimate the magnetic field the clump would have and checking whether it is consistent with that measured in

LMXBs ($B \sim 10^8 - 10^{13}$ G [74, 75]). In Section IV of GC15 we explored the idea of treating the clump of plasma as characterized by some internal force keeping it together, e.g. electrochemical bounds and/or a magnetic force. In Ref. [45] is pointed out that magnetically confined massive clumps of plasma might form in the inner part of the accretion disk. We calculated in equation (9) in GC15 the value of the ratio σ/Y , where σ is the internal force per unit area, $Y = \rho c_s^2$ is the Young's modulus of the material

$$\frac{\sigma}{Y} = \left(\frac{3}{4\pi} \left(\frac{1}{10} \right)^{3/2} \left(1 - \frac{1}{30} \right)^{3/2} \frac{E_b}{Y} \left(\frac{c}{c_s} \right)^3 \times \left(-\frac{2m}{r^3} + \frac{3\tilde{L}^2}{r^4} - \frac{12m\tilde{L}^2}{r^5} \right)^{3/2} \right)^{2/5} \quad (11)$$

Like in solid-state materials, we can think of σ/Y like a hardness of the magnetized clump of plasma. In GC15 we argued that the mechanical binding energy E_b in (11), stored in the clump and keeping it together, should be at least of the same order of that observed in HF QPOs, if the HF QPOs are produced by the tidal disruption of the clump. The amplitude of HF QPOs is some percent the luminosity of the source, i.e. $L_{QPO} \sim 10^{35} - 10^{36}$ erg/s in atoll sources. Following the results in Section III this energy is emitted over a time scale of the order of ~ 0.01 s, thus the energy of the QPO is $E_{QPO} \sim 10^{33} - 10^{34}$ erg. However, this observed energy is only some percent of the total energy emitted. It is the energy modulated by Doppler boosting. For a hot-spot with an over-brightness twice the background disk the modulated energy is only of the order of 1% [22]. Thus, the total energy emitted would be $E_b \sim 10^{36}$ erg. Substituting this E_b in (11) we get $\sigma/Y \sim 300$ for an atoll source with luminosity $L \sim 10^{37}$ erg/s (see also Sec. IV and Sec. VII B in GC15). We can estimate the magnetic field of the clump of plasma. Indeed, if the E_b above is the magnetic binding energy keeping the clump together, then $\sigma = 300Y = 300\rho c_s^2$ is the magnetic pressure $P_m = B^2/2\mu_0$, B the magnetic field and $\mu_0 = 4\pi \times 10^{-7}$ H/m is the magnetic permeability. Equating P_m to σ (in Pascal) we derive a magnetic field permeating the clump of $B \sim 5 \times 10^9$ G. In the case of a Z-source, whose ratio was estimated in GC15 $\sigma/Y \sim 70$, inserting ρ and c_s for a Z-source with luminosity $L \sim 2 \times 10^{38}$ erg/s we get $B \sim 10^{10}$ G, a larger value than atoll sources, as measured [74]. Note however that in Fig. 3 of Ref. [74] atoll sources are located in the region around $B \sim 5 \times 10^8$ G, while Z-sources in that with $B \sim 5 \times 10^9$ G. The discrepancy between these values and those calculated here may be because we did a crude estimation here. For example, we are using the vacuum magnetic permeability $\mu_0 = 4\pi \times 10^{-7}$ H/m, usually also used in plasmas. However, it may be different in the plasma we are dealing with. On the other hand, tidal stretching simulations of the magnetic field in a star [34] show that the magnetic field of the squeezed star strengths at least by a factor

of 10. Thus, if HF QPOs are related to the energy emitted by a magnetic clump of plasma stretched by tides, the estimation of B shown here could give a B actually larger than that of the host LMXB.

Although this result is interesting, giving a B consistent with that measured in NS LMXBs ($B \sim 10^8 - 10^{13}$ G [74, 75]), we would stress that the issues in this section need close attention in dedicated future works.

A. Amplitude of the detectable modulation

Numerical simulations of a hot-spot orbiting around a Kerr black hole and emitting photons show modulations detected as HF QPOs if the hot-spot has some over-brightness with respect to the disk [22]. An over-brightness twice the background disk can give HF QPOs with an amplitude of the order of $\sim 1\%$ the luminosity of the hot-spot. The light curve of the orbiting hot-spot is modulated at the orbital period because of Doppler boosting of the emitted photons, such as relativistic beaming, and gravitational lensing [22]. These relativistic effects magnify the intensity of the electromagnetic radiation emitted. In the case of relativistic beaming, the magnification depends on the velocity of the hot-spot with respect to the observer (see e.g. Ref. [76])

$$I_{\nu(o)} = I_{\nu(e)} D^p \quad (12)$$

where $I_{\nu(o)}$ and $I_{\nu(e)}$ are the observed and emitted specific intensity I_ν , $p = 3 + \alpha$ with α energy spectral index¹¹, D is the Doppler factor

$$D = \frac{1}{\gamma(1 - \beta \cos(\theta))} \quad (13)$$

where $\gamma = 1/\sqrt{(1 - \beta^2)}$ is the Lorentz factor and $\beta = v/c$, with v orbital speed of the clump and c speed of light. Because we are investigating an interval of orbital radii ranging $r \sim 6 - 13 r_g$ it would be worth checking the relative Doppler boosting at $6 r_g$ and $13 r_g$. The Lorentz factor γ and the ratio β at these two radii are $(\beta, \gamma)_{13r_g} = (0.23745, 1.02944)$ and $(\beta, \gamma)_{6r_g} = (0.35482, 1.06959)$. For an edge-on view ($\theta = 0$), inserting in (13) these numbers the relative increment of D^4 is by¹² 67%. Thus, this relative increment affects by 0.67 $I_{\nu(o)}$ any intrinsic trend of $I_{\nu(o)}$ over $r \sim 6 - 13 r_g$.

In Fig. 3 the energy that could be released and possible converted into radiation is in the interval of $2 - 8 \times 10^{35}$ erg, for an atoll source with a luminosity of $L_{atoll} \sim 10^{37}$ erg/s. Over the time-scale the energy is released, ~ 0.01 s, the background energy of the source then is $E_{atoll} \sim 10^{35}$ erg. Therefore, we may have a clump of plasma a

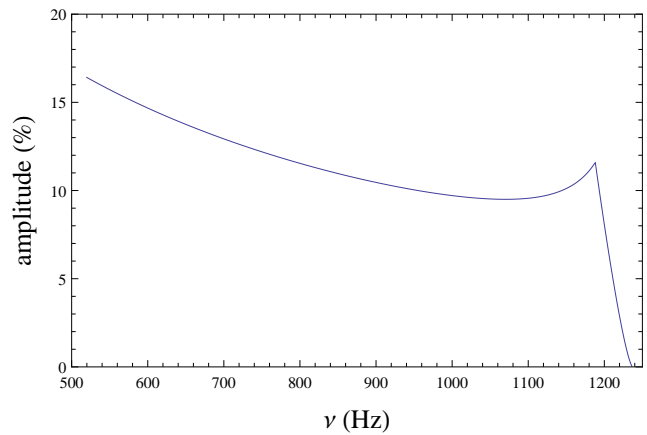


FIG. 5. Amplitude the beat $\nu_k + \nu_r$ would have in the observations after the energy release by tidal circularization of relativistic orbits (Fig. 3). The amplitude is in percent of the luminosity of an atoll NS LMXB ($\sim 10^{37}$ erg/s). The amplitude is plotted as a function of the frequency of the beat $\nu_k + \nu_r$. Such behavior is typical of the amplitude of the upper HF QPO. For a comparison with the data see Fig. 3 in Ref. [52].

factor 8 brighter than the background radiation. Following the results in Ref. [22], in which an over-brightness of the hot-spot by a factor of 2 turns modulations of $\sim 1\%$, we may have modulations up to $\sim 4\%$, i.e. of the order of $\sim 10^{33} - 3 \times 10^{34}$ erg. Thus, the amount of orbital energy released by the clump during tidal circularization of the orbit might give modulations that could be detected at $\nu_k + \nu_r$ in the power spectrum. The mechanism to produce energy proposed here might justify how the orbiting hot-spot would have the over-brightness claimed in other works, in order to produce detectable HF QPOs [21–23].

We divide the modulated fraction of energy by the time-scale the tidal circularization of the orbit takes place, i.e. the time-scale over which the energy is emitted, as a function of the orbital radius. Fig. 5 shows the amplitude the beat $\nu_k + \nu_r$ would have in percent of the luminosity of the source $\sim 10^{37}$ erg/s. Both the value and the behavior in the figure are similar to the upper HF QPO amplitude seen in the observations (Fig. 3 in Ref. [52] (filled stars)), where it is seen to decrease from $\sim 10 - 15\%$ to 1% over the range of frequencies $\sim 500 - 1200$ Hz.

V. DISCUSSION

Several models have been proposed in order to identify the central frequency of the twin-peak HF QPOs with those of the orbital motion around the compact object [20–23, 49, 50, 78]. Some models link the keplerian frequency ν_k of the orbiting matter to the upper peak of the twin-peak HF QPOs, other link ν_k to the lower peak [20, 21, 49, 50]. In Ref. [26] numerical simulations show that tidal disruption of clumps of matter

¹¹ In atoll NS LMXBs $\alpha \geq 1$ (see e.g. Ref. [77])

¹² For an inclination, e.g., $\theta = 50$ the relative magnification drops to 24%.

[25] produces power spectra much alike to the observed ones. The power law and twin-peaks seen in the observations are reproduced. The upper peak corresponds to $\nu_k + \nu_r$, the lower one to ν_k . The light curve of an orbiting clump/hot-spot is drawn by the timing law of its azimuth phase $\phi(t)$. The photons emitted by the clump are cyclically Doppler boosted by relativistic effects and when this happens is dictated by the timing law $\phi(t)$. Because in a curved space-time for non-circular orbits $\nu_r \neq \nu_k$ the different orbital speed at periastron and apastron passage introduces an oscillating term in $\phi(t)$ at the frequency ν_r . In a flat space-time $\phi(t)$ displays this oscillating term as well, but in that case $\nu_r = \nu_k$ and in the power spectra of $\phi(t)$ only the peak at ν_k is seen. In a curved space-time the beats $\nu_k \pm \nu_r$ and ν_k are seen [47]. The beats at $\nu_k \pm \nu_r$ and ν_k are a characteristic of the orbital motion as much as ν_k is in the case of a flat space-time. Therefore, if orbital motion in a curved-space time is producing the twin-peak HF QPOs, it is more natural to link the upper HF QPO to $\nu_k + \nu_r$. This is also what numerical simulations show [26, 47]. It is interesting noting that in the BH LMXB XTE J1550-564 was reported the evidence of a triplet of HF QPOs in a harmonic relationships, 92:184:276 Hz [79]. The one at 92 Hz is the weakest. Individual observations show only a HF QPO, but when averaged together to increase the signal to noise ratio the triplet show up. It is unlikely the same HF QPO is going up and down in frequency since HF QPOs in BH LMXBs are observed at fixed frequencies. Moreover, it would be a really unlikely occurrence the same peak showing up only at these three different orbital radii in integer frequency ratios, 1:2:3. The triplet would fit to the case in which the uppermost peak is the beat $\nu_k + \nu_r$, while the other are ν_k and $\nu_k - \nu_r$ (see also Ref. [47]). The only orbital radius producing the triplet with 92:184:276 Hz is $r_p \sim 7.3 r_g$ for a Schwarzschild black hole with mass $M_{BH} \sim 7.7 M_\odot$. The mass estimated from optical observations is $M_{BH} = 9.10 \pm 0.61 M_\odot$ [80]. Therefore, the pairs of frequency $(\nu_k, \nu_k + \nu_r)$, given by numerical simulations [26], is suitable for interpreting the harmonic relationships of the HF QPOs seen in XTE J1550-564. In Ref. [81] both the mass M_{BH} and dimensionless angular momentum a of the BH LMXB GRO J1655-40 were measured by means of numerical fits, linking ν_k to the upper peak (~ 450 Hz) while $\nu_k - \nu_r$ (periastron precession) to the lower one (~ 300 Hz), as previously proposed by the model [21]. It is not straightforward making a direct comparison of the GRO J1655-40 mass measured in Ref. [81], using the frequency pairs $(\nu_k - \nu_r, \nu_k)$, to that using $(\nu_k, \nu_k + \nu_r)$ as here suggested. In Ref. [81] relativistic frequencies in the Kerr metric were used to fit the data. Also, a third low frequency QPO (~ 18 Hz) linked to the modulation at the nodal precession frequency ν_{nod} was used in the fit. The precession of the plane of the orbit would produce a modulation at ν_{nod} , a general relativistic effect due to frame dragging and known as Lense-Thirring precession [13]. In this manuscript we are using relativistic frequencies of low eccentricity orbits in the

Schwarzschild metric, since here we needed to use exact analytical expressions for both the energy \tilde{E} and angular momentum \tilde{L} for orbits with generic eccentricity e [57]. Moreover, in the Schwarzschild metric the nodes of the orbit do not precess. The mass of GRO J1655-40 from the fit in Ref. [81] agrees with great accuracy to that from optical observations. The best-guess from optical light curves is $M_{BH} = 5.4 \pm 0.3 M_\odot$ [82]. The radius at which the three QPOs would be emitted in Ref. [81] is $r \sim 5.6 r_g$, assuming that the low frequency QPO is the nodal frequency ν_{nod} and not $2\nu_{nod}$ as originally proposed by the model [21]. Using the frequency pairs $(\nu_k, \nu_k + \nu_r)$ to produce twin-peak HF QPOs in a 3:2 ratio, with the lower HF QPO ~ 300 Hz and the upper ~ 450 Hz as in the observations, the mass of the Schwarzschild black hole is $M_{BH} = 4.7 M_\odot$, and the orbital radius where $(\nu_k, \nu_k + \nu_r)$ are in 3:2 ratio is¹³ $r \sim 7.3 r_g$. We emphasize that a precise measurement of the mass of a compact object using the twin-peak HF QPOs is beyond the purpose of this manuscript. It demands close attention and accurate methodology, like that described in Ref. [81].

In Ref. [83] is reported an observational result that could challenge the results presented in this manuscript, i.e. the upper HF QPO corresponding to $\nu_k + \nu_r$ (as numerical simulations [26] and Figs. 4, 5 suggest). The authors studied the behavior of the pulse amplitude in the accreting milliseconds x-ray pulsar SAX J1808.4-3658. It was noted, for the first time, that the pulse amplitude correlates with the frequency (300-700 Hz) of the upper HF QPO detected. It is shown that when the upper HF QPO frequency is below the spin frequency (401 Hz) of the pulsar, the pulse amplitude doubles. When the frequency of the upper HF QPO is above the spin frequency the pulse amplitude halves. This shows evidences on a direct interaction between the spinning magnetosphere of the neutron star and the physical mechanism producing the upper HF QPO. It strongly suggests that the upper HF QPO originates from orbital motion of the plasma in the accretion disk. The possible keplerian nature of the upper HF QPO is highlighted. On the other hand, it is emphasized that the findings also suggest a more general azimuthal nature of the upper HF QPO. It could be keplerian, precessional, or an azimuthally propagating disk wave. If orbital motion is producing the detected upper HF QPO, the findings in Ref. [83] would not discard an upper HF QPO corresponding to the beat $\nu_k + \nu_r$, since this beat is a natural consequence of orbital motion in the curved-space time around the spinning neutron star. It is interesting noting that if the upper HF QPO ranging 300-700 Hz in SAX J1808.4-3658 is the beat $\nu_k + \nu_r$, it would correspond to a range of keplerian frequency

¹³ Note that in the Kerr metric this orbital radius would be $\sim 7 r_g$ for a Kerr black hole with $M_{BH} \sim 5.7 M_\odot$, $a \sim 0.3$. At this radius, the low frequency QPO (~ 18 Hz) used in the fit in Ref. [81] is equal to $2\nu_{nod}$.

$\nu_k \sim 200 - 400$ Hz, i.e. an upper limit equal to the spin frequency of the magnetosphere (401 Hz). The maximum keplerian frequency then is seen at the corotational radius r_c , i.e. the orbital radius at which the keplerian frequency equals the spinning one. In Ref. [84] has been suggested that SAX J1808.4-3658 is near spin equilibrium, i.e. $r_m \sim r_c$, where r_m is the magnetosphere radius. Therefore, a maximum upper HF QPO of ~ 700 Hz might mean a coherent oscillation produced close to or at the magnetosphere radius. Either the disk is truncated at the magnetosphere radius r_m or inside the magnetosphere no coherent oscillations form. Within this interpretation, from the observations [83] we see that as long as the upper HF QPO is produced closer and closer to r_m , the pulse amplitude of the neutron star decreases. Following the arguments in Ref. [83] on centrifugal inhibition, the interpretation of the upper HF QPO equal to the beat $\nu_k + \nu_r$ and, therefore, $\nu_k \sim 200 - 400$ Hz may give suitable arguments. When the plasma in the accretion disk orbits far away the magnetosphere, $r > r_m$, or $\nu_k < \nu_s$, the centrifugal force at the magnetosphere would inhibit this plasma accreting. Therefore, for a clump of plasma orbiting in the disk and producing the upper HF QPO, some plasma of the clump would not be able to flow towards the magnetic poles and would not affect the pulse amplitude. Instead, a clump of plasma orbiting closer to the corotational radius, or close the magnetosphere, thus for keplerian frequencies approaching $\nu_k = 401$ Hz and for $\nu_k + \nu_r$ above 400 Hz, it would be more likely that a fraction of the clump is accreted towards the poles, weakening the pulse amplitude [83]. This interpretation, rather than an upper HF QPO equal to ν_k , might be more suitable for the excursions seen in the pulse amplitude of SAX J1808.4-3658. Such excursions cluster around a frequency of the upper HF QPO of $\sim 600 - 700$ Hz [83], i.e. at $\nu_k \sim 330 - 400$ Hz, close to the frequency at the corotational/magnetosphere radius (401 Hz), where some rest of the clump is more likely to flow to the magnetic poles, causing the pulse amplitude to flicker.

Simultaneous twin-peak HF QPOs in SAX J1808.4-3658 are rarely seen. When HF QPOs were discovered in this source [85], the twin-peaks were detected only in one observation. A systematic study on the variability of SAX J1808.4-3658 has been presented in Ref. [86]. Twin-peak HF QPOs were detected only in three observations (out of many) with different central frequencies. These three detections give clues on the evolution of the twin-peaks frequency. The separation in frequency of the peaks is almost consistent with a constant value (~ 180 Hz) close to half the spin frequency of the pulsar, as previously reported [85]. The highest frequency of the upper HF QPO is ~ 730 Hz yet may be consistent with the fact that the upper HF QPO corresponds to $\nu_k + \nu_r$ and the highest upper HF QPO of ~ 730 Hz is produced at the corotational/magnetosphere radius. On the other hand, a constant separation in frequency of twin-peaks is inconsistent with the pairs $(\nu_k, \nu_k + \nu_r)$, since the difference ν_r varies and does not match the separation mea-

sured. However, a constant separation in frequency is a feature not seen in other atoll sources. The separation usually varies by several tens of hertz with varying central frequency of the peaks [52]. The lower HF QPOs in SAX J1808.4-3658 shows properties that make it to differ than the lower HF QPO in other atoll sources. In SAX J1808.4-3658 the upper HF QPOs is more prominent than the lower [86]. When detected simultaneously, in other atoll sources the lower HF QPO shows a larger amplitude [52, 53]. The coherence $Q \sim 10$ of the lower HF QPO in SAX J1808.4-3658 (of the same order of the upper one) [86] is much lower than in other atoll NS LMXBs, where it can be of the order of $Q \sim 100$ [52, 53]. Calculations in GC15 show that such high coherences may be typical of a keplerian modulation.

If the upper HF QPO in SAX J1808.4-3658 is the beat $\nu_k + \nu_r$ it might justify why its maximum frequency is ~ 700 Hz, since this frequency corresponds to a keplerian frequency almost equal to the spinning one (401 Hz). Therefore, coherent oscillations can form up to the corotational/magnetosphere radius r_m , since the source is in spin equilibrium [84]. Either the disk is truncated at the magnetosphere or inside no coherent modulations form. When the energy of such oscillations is released close to r_m the interaction with the magnetosphere might cause the excursions in pulse amplitude seen in SAX J1808.4-3658 [83]. The lower HF QPO in SAX J1808.4-3658 might be a modulation different than keplerian [6, 85]. It is rarely detected and shows different properties than the lower HF QPO detected in other atoll NS LMXBs.

VI. CONCLUSIONS

The power spectra of LMXBs are characterized by several peaks ranging from low to high frequencies. The highest frequencies detected often show up in pairs, named twin-peak HF QPOs. They have central frequencies typical of the orbital motion of matter close to the compact object [87].

In atoll NS LMXBs the lower and upper HF QPOs show different patterns of their amplitude and coherence versus central frequency [51–54]. The lower HF QPO shows an increase and then a decrease of its both amplitude and coherence. The amplitude of the upper HF QPO keep decreasing with increasing central frequency of the peak. The trend of its coherence remains of the order of $Q \sim 10$ over a large range of frequencies. Following numerical simulations [26], in GC15 we have proposed that the lower twin-peak HF QPO could arise from the energy released during tidal disruption of clumps orbiting in the accretion disk. Here we have wondered whether the energy and coherence observed in the upper HF QPO could originate because of the tidal circularization of the clump's orbit. The tidal force acting on an orbiting clump circularizes and shrinks the orbit and the clump emits the released orbital energy as radiation [43]. The modulation at $\nu_k + \nu_r$ caused by the eccentricity of the

orbit [47] should originate because of the energy released in the phase of tidal circularization of the orbit. We have estimated the energy that clumps of plasma orbiting in the accretion disk would release because of tidal circularization of their relativistic orbits. We note for the first time that such physical mechanism might account for the amplitude and coherence of the upper HF QPO observed in atoll NS LMXBs (Figs. 2, 3 of Ref. [52]). Numerical simulations [26, 47], the results presented here (Figs. 4, 5) and the discussion on SAX J1808.4-3658 suggest that the upper HF QPO most probably corresponds to the beat $\nu_k + \nu_r$.

The physical mechanism to release energy proposed here, together with the modulation mechanism in

Refs. [22, 23, 26, 47], might offer an explanation on why the upper HF QPO would originate. This work might be the first time we are recognizing the tidal circularization of relativistic orbits occurring around a neutron star.

ACKNOWLEDGMENTS

I would like to thank Rodolfo Casana, Manoel M. Ferreira Jr., Adalto R. Gomes and Alessandro Patruno for discussions on the topic. I thank the anonymous referees for valuable comments that helped to improve the manuscript. This work was fully supported by the program PNPB/CAPES-Brazil.

-
- [1] F. K. Lamb, in *From X-ray Binaries to Gamma-Ray Bursts: Jan van Paradijs Memorial Symposium*, Astronomical Society of the Pacific Conference Series, Vol. 308, edited by E. P. van den Heuvel, L. Kaper, E. Rol, and R. A. M. J. Wijers (2003) p. 221, arXiv:0705.0030.
- [2] M. van der Klis, J. H. Swank, W. Zhang, K. Jahoda, E. H. Morgan, W. H. G. Lewin, B. Vaughan, and J. van Paradijs, *ApJ* **469**, L1 (1996), arXiv:astro-ph/9607047.
- [3] R. A. Remillard and J. E. McClintock, *ARA&A* **44**, 49 (2006), astro-ph/0606352.
- [4] T. M. Belloni and S. E. Motta, *Astrophysics of Black Holes: From Fundamental Aspects to Latest Developments*, *A&A* **540**, 61 (2016), arXiv:1603.07872 [astro-ph.HE].
- [5] M. A. Abramowicz and W. Kluźniak, *A&A* **374**, L19 (2001), arXiv:astro-ph/0105077.
- [6] W. Kluźniak, M. A. Abramowicz, S. Kato, W. H. Lee, and N. Stergioulas, *ApJ* **603**, L89 (2004), astro-ph/0308035.
- [7] P. Rebusco, *Astronomische Nachrichten* **326**, 830 (2005), astro-ph/0510419.
- [8] J. Horák and V. Karas, *A&A* **451**, 377 (2006), astro-ph/0601053.
- [9] Z. Stuchlík, A. Kotrlová, and G. Török, *A&A* **552**, A10 (2013), arXiv:1305.3552 [astro-ph.HE].
- [10] M. van der Klis, *ArXiv Astrophysics e-prints* (2004), astro-ph/0410551.
- [11] S. E. Motta, A. Rouco-Escorial, E. Kuulkers, T. Muñoz-Darias, and A. Sanna, *MNRAS* **468**, 2311 (2017), arXiv:1703.01263 [astro-ph.HE].
- [12] L. Stella and M. Vietri, *ApJ* **492**, L59 (1998), astro-ph/9709085.
- [13] J. Lense and H. Thirring, *Physikalische Zeitschrift* **19** (1918).
- [14] A. Ingram, M. van der Klis, M. Middleton, C. Done, D. Altamirano, L. Heil, P. Uttley, and M. Axelsson, *MNRAS* **461**, 1967 (2016), arXiv:1607.02866 [astro-ph.HE].
- [15] A. Ingram, M. van der Klis, M. Middleton, D. Altamirano, and P. Uttley, *MNRAS* **464**, 2979 (2017), arXiv:1610.00948 [astro-ph.HE].
- [16] M. van der Klis, M. Dooburgh and M. van der Klis, *MNRAS* **465**, 3581 (2017), arXiv:1611.05860 [astro-ph.HE].
- [17] K. Schwarzschild, *Abh. Konigl. Preuss. Akad. Wissenschaften Jahre 1906,92*, Berlin,1907 **1916**, 189 (1916).
- [18] C. W. Misner, K. S. Thorne, and J. A. Wheeler, *Gravitation*, *W. H. Freeman & Company, San Francisco*. (1973).
- [19] W. Kluźniak, P. Michelson, and R. V. Wagoner, *ApJ* **358**, 538 (1990).
- [20] M. C. Miller, F. K. Lamb, and D. Psaltis, *ApJ* **508**, 791 (1998), arXiv:astro-ph/9609157.
- [21] L. Stella, M. Vietri, and S. M. Morsink, *ApJ* **524**, L63 (1999), arXiv:astro-ph/9907346.
- [22] J. D. Schnittman and E. Bertschinger, *ApJ* **606**, 1098 (2004), arXiv:astro-ph/0309458.
- [23] J. D. Schnittman, G. D. Öfrik (2016), Karas, M. Dovčiak, M. Wildner, D. Wzientek, E. Šrámková, M. Abramowicz, K. Goluchová, G. P. Mazur, and F. H. Vincent, *MNRAS* **439**, 1933 (2014), arXiv:1401.4468 [astro-ph.HE].
- [24] A. Čadež and U. Kostić, *Phys. Rev. D* **72**, 104024 (2005), gr-qc/0405037.
- [25] U. Kostić, A. Čadež, M. Calvani, and A. Gomboc, *A&A* **496**, 307 (2009), arXiv:0901.3447 [astro-ph.HE].
- [26] C. Germanà, U. Kostić, A. Čadež, and M. Calvani, in *American Institute of Physics Conference Series*, American Institute of Physics Conference Series, Vol. 1126, edited by J. Rodriguez and P. Ferrando (2009) pp. 367–369, arXiv:0902.2134 [astro-ph.HE].
- [27] J. Guillochon, H. Manukian, and E. Ramirez-Ruiz, *ApJ* **783**, 23 (2014), arXiv:1304.6397 [astro-ph.HE].
- [28] J. M. Miller, J. S. Kaastra, M. C. Miller, M. T. Reynolds, G. Brown, S. B. Cenko, J. J. Drake, S. Gezari, J. Guillochon, K. Gultekin, J. Irwin, A. Levan, D. Maitra, W. P. Maksym, R. Mushotzky, P. O’Brien, F. Paerels, J. de Plaa, E. Ramirez-Ruiz, T. Strohmayer, and N. Tanvir, *Nature* **526**, 542 (2015), arXiv:1510.06348 [astro-ph.HE].
- [29] S. Komossa, *Journal of High Energy Astrophysics* **7**, 148 (2015), arXiv:1505.01093 [astro-ph.HE].
- [30] D. Lin, O. Godet, L. C. Ho, D. Barret, N. A. Webb, and J. A. Irwin, *MNRAS* **468**, 783 (2017), arXiv:1702.06956 [astro-ph.HE].
- [31] A. Gomboc and A. Čadež, *ApJ* **625**, 278 (2005), astro-ph/0502507.
- [32] L. Dai, J. C. McKinney, and M. C. Miller, *ApJ* **812**, L39 (2015), arXiv:1507.04333 [astro-ph.HE].
- [33] C. Bonnerot, E. M. Rossi, and

- G. Lodato, MNRAS **464**, 2816 (2017), arXiv:1608.00970 [astro-ph.HE].
- [34] C. Bonnerot, D. J. Price, G. Lodato, and E. M. Rossi, MNRAS **469**, 4879 (2017), arXiv:1611.09853 [astro-ph.HE].
- [35] R. C. Reis, J. M. Miller, M. T. Reynolds, K. Gültekin, D. Maitra, A. L. King, and T. E. Strohmayer, Science **337**, 949 (2012), arXiv:1208.1046 [astro-ph.CO].
- [36] E. Bozzo, A. Papitto, C. Ferrigno, and T. M. Belloni, A&A **570**, L2 (2014), arXiv:1409.6664 [astro-ph.HE].
- [37] S. J. Peale, P. Cassen, and R. T. Reynolds, Science **203**, 892 (1979).
- [38] J. H. Roberts and F. Nimmo, Icarus **194**, 675 (2008).
- [39] L. Iess, D. J. Stevenson, M. Parisi, D. Hemingway, R. A. Jacobson, J. I. Lunine, F. Nimmo, J. W. Armstrong, S. W. Asmar, M. Ducci, and P. Tortora, Science **344**, 78 (2014).
- [40] C. J. Hansen, L. Esposito, A. I. F. Stewart, J. Colwell, A. Hendrix, W. Pryor, D. Shemansky, and R. West, Science **311**, 1422 (2006).
- [41] D. Shoji, H. Hussmann, F. Sohl, and K. Kurita, Icarus **235**, 75 (2014).
- [42] A. Rodríguez, S. Ferraz-Mello, T. A. Michtchenko, C. Beaugé, and O. Miloni, MNRAS **415**, 2349 (2011), arXiv:1104.0964 [astro-ph.EP].
- [43] A. Čadež, M. Calvani, and U. Kostić, A&A **487**, 527 (2008), arXiv:0809.1783.
- [44] A. Čadež, U. Kostić, and M. Calvani, in *American Institute of Physics Conference Series*, American Institute of Physics Conference Series, Vol. 1205, edited by R. Ruffini and G. Vereshchagin (2010) pp. 30–40, arXiv:0908.0117 [astro-ph.HE].
- [45] S. Horn and W. Kundt, Ap&SS **158**, 205 (1989).
- [46] C. J. Skipper, I. M. McHardy, and T. J. Maccarone, MNRAS **434**, 574 (2013), arXiv:1306.2475 [astro-ph.HE].
- [47] C. Germanà, MNRAS **430**, L1 (2013), arXiv:1211.3344 [astro-ph.HE].
- [48] V. Osherovich and L. Titarchuk, ApJ **522**, L113 (1999), astro-ph/9907360.
- [49] L. Titarchuk and V. Osherovich, ApJ **518**, L95 (1999), astro-ph/9904293.
- [50] B. Mukhopadhyay, S. Ray, J. Dey, and M. Dey, ApJ **584**, L83 (2003), astro-ph/0211611.
- [51] M. Méndez, M. van der Klis, and E. C. Ford, ApJ **561**, 1016 (2001), astro-ph/0006245.
- [52] D. Barret, J.-F. Olive, and M. C. Miller, MNRAS **370**, 1140 (2006), arXiv:astro-ph/0605486.
- [53] M. Méndez, MNRAS **371**, 1925 (2006), astro-ph/0607433.
- [54] D. Barret, M. Bachetti, and M. C. Miller, ApJ **728**, 9 (2011).
- [55] G. Hasinger and M. van der Klis, A&A **225**, 79 (1989).
- [56] C. Germanà and R. Casana, Phys. Rev. D **91**, 083013 (2015), arXiv:1504.02397 [astro-ph.HE].
- [57] C. Cutler, D. Kennefick, and E. Poisson, Phys. Rev. D **50**, 3816 (1994).
- [58] J. F. Hawley and J. H. Krolik, ApJ **548**, 348 (2001), astro-ph/0006456.
- [59] J. M. Corral-Santana, J. Casares, T. Muñoz-Darias, P. Rodríguez-Gil, T. Shahbaz, M. A. P. Torres, C. Zurita, and A. A. Tyndall, Science **339**, 1048 (2013), arXiv:1303.0034 [astro-ph.GA].
- [60] A. Ingram and M. van der Klis, MNRAS **434**, 1476 (2013), arXiv:1306.3823 [astro-ph.HE].
- [61] A. R. Ingram, Astronomische Nachrichten **337**, 385 (2016), arXiv:1511.07181 [astro-ph.HE].
- [62] S. S. Kokarev, Nuovo Cimento B Serie **124**, 155 (2009), arXiv:0810.5262 [gr-qc].
- [63] J. Frank, A. King, and D. J. Raine, *Accretion Power in Astrophysics, by Juhan Frank and Andrew King and Derek Raine, pp. 398. ISBN 0521620538. Cambridge, UK: Cambridge University Press, February 2002.* (2002).
- [64] A. Sanna, M. Méndez, D. Altamirano, J. Homan, P. Casella, T. Belloni, D. Lin, M. van der Klis, and R. Wijnands, MNRAS **408**, 622 (2010), arXiv:1005.3217 [astro-ph.HE].
- [65] W. H. Press and S. A. Teukolsky, ApJ **213**, 183 (1977).
- [66] M. Berger, M. van der Klis, J. van Paradijs, W. H. G. Lewin, F. Lamb, B. Vaughan, E. Kuulkers, T. Augusteijn, W. Zhang, F. E. Marshall, J. H. Swank, I. Lapidus, J. C. Lochner, and T. E. Strohmayer, ApJ **469**, L13 (1996).
- [67] R. Popham and R. Sunyaev, ApJ **547**, 355 (2001), astro-ph/0004017.
- [68] A. Sanna, B. Hiemstra, M. Méndez, D. Altamirano, T. Belloni, and M. Linares, MNRAS **432**, 1144 (2013), arXiv:1303.6337 [astro-ph.HE].
- [69] H. C. Lee, R. Misra, and R. E. Taam, ApJ **549**, L229 (2001), astro-ph/0102209.
- [70] M. Gilfanov and M. Revnivtsev, Astronomische Nachrichten **326**, 812 (2005), astro-ph/0512361.
- [71] E. M. Ribeiro, M. Méndez, G. Zhang, and A. Sanna, MNRAS **471**, 1208 (2017), arXiv:1707.03200 [astro-ph.HE].
- [72] J. D. Schnittman, in *22nd Texas Symposium on Relativistic Astrophysics*, edited by P. Chen, E. Bloom, G. Madejski, and V. Patrosian (2005) pp. 511–516, astro-ph/0502048.
- [73] L.-H. Yan and J.-C. Wang, Research in Astronomy and Astrophysics **11**, 631 (2011).
- [74] D. Psaltis and F. K. Lamb, Astronomical and Astrophysical Transactions **18**, 447 (1999).
- [75] M. Revnivtsev and S. Mereghetti, Space Sci. Rev. **191**, 293 (2015), arXiv:1411.5843 [astro-ph.HE].
- [76] K. I. Kellermann, Y. Y. Kovalev, M. L. Lister, D. C. Homan, M. Kadler, M. H. Cohen, E. Ros, J. A. Zensus, R. C. Vermeulen, M. F. Aller, and H. D. Aller, Ap&SS **311**, 231 (2007), arXiv:0708.3219.
- [77] L. Titarchuk and N. Shaposhnikov, ApJ **626**, 298 (2005), astro-ph/0503081.
- [78] G. Török, K. Goluchová, J. Horák, E. Šrámková, M. Urbanec, T. Pecháček, and P. Bakala, MNRAS **457**, L19 (2016), arXiv:1512.03841 [astro-ph.HE].
- [79] R. A. Remillard, M. P. Muno, J. E. McClintock, and J. A. Orosz, ApJ **580**, 1030 (2002), astro-ph/0202305.
- [80] J. A. Orosz, J. F. Steiner, J. E. McClintock, M. A. P. Torres, R. A. Remillard, C. D. Bailyn, and J. M. Miller, ApJ **730**, 75 (2011), arXiv:1101.2499 [astro-ph.SR].
- [81] S. E. Motta, T. M. Belloni, L. Stella, T. Muñoz-Darias, and R. Fender, MNRAS **437**, 2554 (2014), arXiv:1309.3652 [astro-ph.HE].
- [82] M. E. Beer and P. Podsiadlowski,

- MNRAS **331**, 351 (2002), astro-ph/0109136.
- [83] P. Bult and M. van der Klis, ApJ **798**, L29 (2015), arXiv:1501.00791 [astro-ph.HE].
- [84] J. M. Hartman, A. Patruno, D. Chakrabarty, D. L. Kaplan, C. B. Markwardt, E. H. Morgan, P. S. Ray, M. van der Klis, and R. Wijnands, ApJ **675**, 1468-1486 (2008), arXiv:0708.0211.
- [85] R. Wijnands, M. van der Klis, J. Homan, D. Chakrabarty, C. B. Markwardt, and E. H. Morgan, Nature **424**, 44 (2003), astro-ph/0307123.
- [86] P. Bult and M. van der Klis, ApJ **806**, 90 (2015), arXiv:1505.00596 [astro-ph.HE].
- [87] J. Wang, International Journal of Astronomy and Astrophysics **6**, 82